



## UPLC-QTOF/MS-assisted chemical profiling of *Daucus carota* leaf extract and evaluation of its antioxidant, antimicrobial and antibiofilm activities: Evidence from *in vitro* and *in silico* studies

Hayam N.S. Mahmoud<sup>a</sup>, Maha A.M. El-Shazly<sup>b,\*</sup>, Amal M. Saad<sup>b</sup>, Laila A. Refahy<sup>b</sup>, Mosad A. Ghareeb<sup>b</sup>, Sameh Rizk<sup>a</sup>



<sup>a</sup> Chemistry Department, Faculty of Science, Ain Shams University, Abbasiya, Cairo 11566, Egypt

<sup>b</sup> Medicinal Chemistry Department, Theodor Bilharz Research Institute, Kornaish El Nile, Warrak El-Hadar, Imbaba, Giza 12411, Egypt

### Abstract

The current study aims to evaluate the antioxidant, antimicrobial and antibiofilm activities of different extracts of Carrot (*Daucus carota* L.) leaves as well as their total phenolic content (TPC). Also, the chemical profiling of the most promising extract was performed using UPLC-MS/MS analysis in a negative ion mode. In the DPPH assay, the IC<sub>50</sub> values were ranged from 28.07 to 71.58 µg/ml, while in the phosphomolybdenum assay the total antioxidant capacity (TAC) values were ranged from 34.0 to 314.67 mg AAE/g dry extract. The antioxidant results were supported by the TPC findings which were ranged from 13.40 to 144.56 GAE/g dry extract. The tested extracts showed variable antimicrobial effects against four pathogenic microbial strains including *Staphylococcus aureus* (0-15 mm), *Escherichia coli* (0-13 mm), *Candida albicans* (0-11 mm) and *Aspergillus niger* (0-8 mm). While, the antibiofilm inhibitory effect was evaluated against *Escherichia coli*, *Staphylococcus aureus*, *Bacillus subtilis* and *Pseudomonas aeruginosa* with inhibition ratio (%) range of 0-55.26, 0-60.23, 0-40.25, and 0-32.23, respectively. The chemical characterization of the *n*-butanol as the most potent antioxidant extract led to the identification of 34 compounds and the majority of the identified compounds were categorized as phenolic acids and flavonoids. Following an *in silico* investigation of the annotated compounds, caffeic and iso-ferulic acids were putatively characterized as probable inhibitors of pyruvate kinase, through which they exert the extract's antibacterial effect. To sum up, Carrot leaves are a promising source of natural antioxidant and antimicrobial compounds that can be used in the development of pharmaceutical industries.

**Keywords:** *Daucus carota* L.; antioxidant; antimicrobial; antibiofilm; UPLC-MS/MS; docking; molecular dynamics simulation

### 1. Introduction

*Daucus* genus (family: Apiaceae) comprise about 600 species, where it spreads all over the world. The genus is native to Europe, Asia and Africa. Carrot (*D. carota* L.) is an edible vegetable and is mainly used as a food source for humans due to its important nutrients. Traditionally, the plant has been used for the treatment of several ailments including hepatic & renal insufficiency, skin disorders, infectious disease and diarrhea [1-3]. Different Carrot extracts have been

evaluated for their antioxidants, antifungal and antibacterial activities [4,5]. Phytochemically, the volatile oil consisted of numerous chemical ingredients like monoterpenes, sesquiterpenes, and phenylpropanoids [6-8]. Also, previous phytochemical investigations were carried out on different *Daucus* species revealed the presence of a broad array of chemical categories *viz.*, alkaloids, carbohydrates, flavonoids, phenolic acids, terpenoids and coumarins [9].

Medicinal plants, especially edible ones, are an important source of bioactive compounds that are

\*Corresponding author e-mail: m.elshazly@tbri.gov.eg.; (Maha A. M. Elshazly).

Received date 05 May 2023; revised date 17 May 2023; accepted date 21 May 2023

DOI: 10.21608/EJCHEM.2023.209102.7935

©2023 National Information and Documentation Center (NIDOC)

used as naturally occurring antioxidants [10]. Antioxidants are compounds capable of scavenging free radicals and delaying the oxidation of oxidizable substances [11]. Free radicals are molecules with high energy that have the ability to interact with tissues inside the human body, causing serious health damage, and excessive free radicals lead to what is known as oxidative stress [12].

Recently, infectious microbial diseases have spread rapidly due to the resistance of some microbial species to antibiotics, and the world is now in urgent need to discover new and effective drugs against microbes, so scientists tended to discover antimicrobial drugs from safe natural sources like medicinal plants [13].

A biofilm is a complex group of closely related microorganisms that adhere to biotic and abiotic surfaces. Biofilms are formed as a result of the formation of a viscous gel of sugars, proteins and organic matter on wet surfaces. Biofilms contain the most antibiotic-resistant bacteria [14,15]. Therefore, this study discusses the antioxidant, antimicrobial and antibiofilm of different extracts of *D. carota* L. leaves in addition to chemical profiling of the promising extract using UPLC-MS/MS analysis.

## 2. Materials and Methods

### 2.1. Plants materials

The fresh leaves of *D. carota* L. plant were collected from a farm in Qalyubiyya Governorate, Egypt, during February 2020. The plant was identified by specialists in the herbarium of the Botany Department, Faculty of Science, Cairo University. A voucher specimen (Da.L.\_2020) was preserved in the herbarium of the Medicinal Chemistry Department, Theodor Bilharz Research Institute. The plant materials were dried in the shade at room temperature and then ground using a grinding machine.

### 2.2. Extraction and fractionation

The air-dried leaves of *D. carota* (1.5 kg) were extracted with methanol (4 liters x 3 times) by soaking at room temperature. The solvent was evaporated using rotatory evaporator (BUCHI R-300, Switzerland) under vacuum at 40 °C, the dry residue (252g: 16.8%) was fractionated using organic solvents like petroleum ether (60-80 °C), dichloromethane, ethyl acetate, and *n*-butanol to afford petroleum ether (35 g: 2.33%), dichloromethane (3.35 g: 0.22%), ethyl acetate (4.6

g: 0.31%), *n*-butanol (30 g: 2.0%) and water extracts (134.12 g: 8.94%).

### 2.3. Antioxidant activity evaluation

#### 2.3.1. Free radical scavenging activity using DPPH assay

The free radical scavenging antioxidant activity was assessed using DPPH assay according to the reported procedures with simple modifications [16].

#### 2.3.2. Phosphomolybdenum assay

The total antioxidant capacity (TAC) was estimated using phosphomolybdenum test according to the reported procedures [17].

### 2.4. Total phenolic content estimation

The total phenolic content was estimated using Folin-Ciocalteu's assay according to the previously described method [18].

### 2.5. Antimicrobial activity evaluation

The *in vitro* antimicrobial activity was evaluated using disc agar diffusion method according to the reported procedures [19,20].

### 2.6. Antibiofilm activity evaluation

The biofilm inhibitory activity was evaluated using microtiter plate assay (MTP) according to the reported procedures [21].

### 2.7. Molecular modeling studies (Supplementary file) [22-28]

### 2.8. Statistical analysis

All data were presented as mean  $\pm$  S.D. using SPSS 13.0 program (SPSS Inc. USA).

## 3. Results and Discussion

### 3.1. Total phenolic content (TPC) and antioxidant activities

Free radicals are highly energetic molecules that when accumulated within the tissues of a living body led to generation of several abnormal phenomena like oxidative stress. It also causes many serious diseases such as cancer, cardiovascular, and inflammation. Moreover, the harmful effects of this phenomenon can be diminished via using naturally occurring antioxidant compounds as free radical scavengers [29-32]. Therefore, the different solvent extracts of *D. carota* leaves were screened for their antioxidant activity. As illustrated in table 1, *D. carota* leaf methanolic extract exhibited a total phenolic content (TPC) equal to 106.63 mg GAE/g dry extract. Moreover, the TPC values of its derived sub-fractions are in the order: *n*-BuOH (144.56) > EtOAc (113.95) > H<sub>2</sub>O (69.65) > CH<sub>2</sub>Cl<sub>2</sub> (32.10) > Pet. ether (13.40) (Table 1). On the other side, the antioxidant activity

was assayed via using two antioxidant assays namely 2,2-diphenyl-1-picrylhydrazyl (DPPH) and phosphomolybdenum. In the DPPH assay, the *D. carota* leaf methanolic extract exhibited free radical scavenging activity with IC<sub>50</sub> value of 40.75 µg/ml, while its derived fraction showed variable activities with IC<sub>50</sub> value of 28.07, 32.24, and 71.58 µg/ml, respectively for *n*-BuOH, EtOAc, and H<sub>2</sub>O fractions compared with ascorbic acid as a positive control with IC<sub>50</sub> value of 7.39 µg/ml. There is no activity was recorded with petroleum ether and CH<sub>2</sub>Cl<sub>2</sub> fractions (Table 1). While in the phosphomolybdenum assay, the methanol extract displayed total antioxidant capacity (TAC) value of 256.0 mg AAE/g dry extract and for its derived fraction the TAC values are in the order: *n*-BuOH (314.67) > EtOAc (282.32) > 154.0 (69.65) > CH<sub>2</sub>Cl<sub>2</sub> (52.0) > Pet. ether (34.0) mg AAE/g dry

extract (Table 1). Previous reports stated that the different parts of *D. carota* showed promising antioxidant activities which correlated to their phenolic composition. For instance, the methanol, ethyl acetate and hexane extracts from *D. carota* aerial parts grown in Nigeria showed antioxidant activity with EC<sub>50</sub> values of 86.89, 166.79, and 490.74 µg/ml, respectively<sup>[33]</sup>. Generally, phenolic compounds have a high ability to scavenge free radicals and reach a balance between internal antioxidants and oxidative stress resulting from the accumulation of free radicals inside the body. The mechanism of action of phenolic compounds as antioxidants depends on the presence of a heavy number of hydroxyl groups, keto groups, carboxylic groups and extended conjugation<sup>[34-36]</sup>.

Table 1: DPPH free radical antioxidant activity, total antioxidant capacity (TAC) and total phenolic content (TPC) of *D. carota* leaf extract as well as its derived fractions.

Sample	Total phenolic content (mg GAE/g dry extract) <sup>1,2</sup>	DPPH free radical antioxidant activity (IC <sub>50</sub> µg/ml) <sup>3</sup>	Total antioxidant capacity (mg AAE/g dry extract) <sup>4</sup>
MeOH	106.63 ± 3.27	40.75 ± 0.82	256.0 ± 2.0
Pet. ether	13.40 ± 3.07	> 100	34.0 ± 3.23
CH <sub>2</sub> Cl <sub>2</sub>	32.10 ± 2.19	> 100	52.0 ± 1.75
EtOAc	113.95 ± 2.36	32.24 ± 0.42	282.32 ± 2.03
<i>n</i> -BuOH	144.56 ± 1.18	28.07 ± 0.19	314.67 ± 3.05
H <sub>2</sub> O	69.65 ± 2.49	71.58 ± 0.15	154.0 ± 2.0
Ascorbic acid	-	7.39 ± 1.52	-

<sup>1</sup>Results are (means ± S.D.) (n = 3); <sup>2</sup>GAE (gallic acid equivalent); <sup>3</sup>IC<sub>50</sub>: The amount of extract needed to scavenge 50% of DPPH radicals; <sup>4</sup>AAE (ascorbic acid equivalent).

### 3.2. Antimicrobial activity

Natural products have a long history in treating and combating infectious microbial diseases due to their diverse and unique chemical composition<sup>[37-40]</sup>. Herein, the methanol extract of *D. carota* leaves and its derived sub-fractions were evaluated for their antimicrobial activities against some pathogenic microbial strains. The results presented in table 2 reveals that the antimicrobial inhibition zones were ranged from 0 to 15 mm, 0 to 13 mm, 0 to 11 mm and 0 to 8 mm, respectively against *S. aureus* against six pathogenic microbial strains including *Pseudomonas aeruginosa*, *Escherichia coli*, *Staphylococcus aureus*, *Micrococcus luteus*, *Candida albicans*, and *Candida tropicalis* with inhibition zone

*aureus*, *E. coli*, *C. albicans* and *A. niger*. Also, we can concluded that the ethyl acetate fraction is the most potent fraction against all tested microorganisms; *S. aureus* (15 mm) compared to Ciprofloxacin (18 mm), *E. coli* (13 mm) compared to Ciprofloxacin (19 mm), *C. albicans* (11 mm) compared to Nystatin (18 mm) and *A. niger* (8 mm) compared to Nystatin (17 mm). Our current findings were matched to some extent of the previous studies, the ethanolic extract from *D. carota* canopy grown in Egypt showed antimicrobial values of 5.49, 3.39, 20.2, 12.61, 9.21, 6.61 mm, respectively<sup>[41]</sup>. Previous reports indicated that phenolic compounds possess superior antimicrobial efficacy, and due to the diversity of their chemical

composition, their mechanism of action as antimicrobials varies greatly [42]. The mechanism of action of phenolic compounds as antimicrobials includes "inhibition of nucleic acid synthesis, inhibition of cytoplasmic membrane function,

inhibition of energy metabolism, attenuation of the pathogenicity, inhibition of biofilm development, alteration of the membrane permeability [43,44].

Table 2: Antimicrobial effect of different extracts of *D. carota*.

Sample	<i>Staphylococcus aureus</i>	<i>Escherichia coli</i>	<i>Candida albicans</i>	<i>Aspergillus niger</i>
MeOH	13.00mm	12.00mm	0.00mm	0.00mm
<i>n</i> -BuOH	0.00mm	0.00mm	0.00mm	0.00mm
CH <sub>2</sub> Cl <sub>2</sub>	9.00mm	10.00mm	0.00mm	0.00mm
EtOAc	15.00mm	13.00mm	11.00mm	8.00mm
Pet. ether	9.00mm	8.00mm	0.00mm	0.00mm
H <sub>2</sub> O	0.00mm	0.00mm	0.00mm	0.00mm
Nys	-	-	18.00mm	17.00mm
Cip	18.00mm	19.00mm	-	-

Nys: Nystatin; Cip: Ciprofloxacin.

### 3.3. Antibiofilm activity

The methanol extract of *D. carota* leaves and its sub-derived fractions were screened for their antibiofilm inhibitory effects against some pathogenic microbial strains. The results presented in **table 3** showed that the methanol, dichloromethane, ethyl acetate and *n*-butanol extracts exhibited variable inhibitory effects, while there is no any activity was recorded in case of petroleum ether and water extracts. The inhibitory effects were ranged from 23.23 to 55.26 %, 0 to 60.23%, 0 to 40.25 % and 0 to 32.23 %, respectively against *E. coli*, *S. aureus*, *B. subtilis* and *P. aeruginosa*. To the best of our knowledge, there is no available information in the literature about the antibiofilm activity of *D. carota* leaf extracts. It was reported that the plant phytoconstituents have the ability to act as antibiofilm agents via various modes of action including "adhesion, inhibition of quorum-sensing, and motility" [45].

respectively against *E. coli*, *S. aureus*, *B. subtilis* and *P. aeruginosa*. To the best of our knowledge, there is no available information in the literature about the antibiofilm activity of *D. carota* leaf extracts. It was reported that the plant phytoconstituents have the ability to act as antibiofilm agents via various modes of action including "adhesion, inhibition of quorum-sensing, and motility" [45].

Table 3:Antibiofilm activity of different extracts of *D. carota* against *P. aeruginosa*, *S. aureus*, *E. coli* and *B. subtilis*.

Sample	Inhibition ratio (%)			
	<i>E. coli</i>	<i>S. aureus</i>	<i>B. subtilis</i>	<i>P. aeruginosa</i>
MeOH	37.20	0.00	12.00	0.00
<i>n</i> -BuOH	30.25	10.25	16.00	0.00
CH <sub>2</sub> Cl <sub>2</sub>	23.23	17.65	26.33	32.23
EtOAc	55.26	60.23	40.25	14.25
Pet. ether	0.00	0.00	0.00	0.00
H <sub>2</sub> O	0.00	0.00	0.00	0.00

### 3.4. UPLC-QTOF-MS/MS analysis of the *n*-butanol extract of *D. carota* leaves

UPLC coupled with a high resolution mass spectrometry (MS/MS) is a successful technique for rapid identification of large number of chemical compounds; it gives accurately the exact mass, formulae and differentiates between isomeric compounds [46-49]. In the current study, the *n*-butanol as a polyphenolic-rich extract was explored for its chemical constituents using UPLC-QTOF-MS/MS

analysis in a negative ion mode. The analysis led to the identification of 34 compounds based on their retention times, fragmentation patterns and via comparison with the available reported data. The identified compounds were categorized as carboxylic acids, phenolic acids, flavonoids, benzene derivatives, coumarins, anthraquinones, steroids, cholestanoids, benzaldehydes, phenols and fatty acids (Figures 1 & 1S and Table 4). The

phenolic acids and flavonoids were the dominant compounds in the extract.

### 3.4.1. Phenolic and organic acids

A signal demonstrated an [M-H]- $m/z$  at 191 and daughter ions at 173 [M-H-H<sub>2</sub>O]-, 127, 109, 93, and 85; it was tentatively identified as quinic acid [29]. A signal demonstrated an [M-H]- $m/z$  at 133 and daughter ions at 115 [M-H-H<sub>2</sub>O]-, 87, and 71; it was tentatively identified as malic acid [29]. A signal showed an [M-H]- $m/z$  at 115 and a daughter ion at 71 [M-H-CO<sub>2</sub>]-; it was tentatively identified as maleic acid [50]. A signal demonstrated an [M-H]- $m/z$  at 137 and daughter ions at 109 [M-H-CO]-, 108 [M-2H-CO]-, 93 [M-H-CO<sub>2</sub>]-, 92 [M-2H-CO<sub>2</sub>]-, 81, and 65; it was tentatively identified as 3-hydroxybenzoic acid [51]. A signal demonstrated an [M-H]- $m/z$  at 167 and daughter ions at 153 [M-H-CH<sub>2</sub>]-, 152 [M-H-CH<sub>3</sub>]-, 123 [M-H-CO<sub>2</sub>]-, 109 [M-H-CH<sub>3</sub>-CO<sub>2</sub>]-, 108 [M-2H-CH<sub>3</sub>-CO<sub>2</sub>]-, 91 [M-H-COOH-OCH<sub>3</sub>]-, 73 and 65; it was tentatively identified as vanillic acid [52]. A signal demonstrated an [M-H]- $m/z$  at 179 and daughter ions at 135 [M-H-CO<sub>2</sub>]-, and 107 [M-H-CO<sub>2</sub>-CO]-; it was tentatively identified as caffeic acid [53]. A signal demonstrated an [M-H]- $m/z$  at 353 and daughter ions at 191 [M-H-caffeic acid moiety]-, 179 [M-H-quinic acid moiety]-, 161, 135 and 85; it was tentatively identified as neochlorogenic acid [54]. A signal demonstrated an [M-H]- $m/z$  at 515 and daughter ions at 353 [M-H-caffeic acid moiety]-, 191 [M-H-2caffeic acid moiety]-, 179 [M-H-caffeic acid moiety-quinic acid moiety]-, 173, 161, and 135; it was tentatively identified as 1,5-dicaffeoylquinic acid [55]. A signal demonstrated an [M-H]- $m/z$  at 515 and a daughter ion at 353 [M-H-caffeic acid moiety]-; it was tentatively identified as 3,5-di-O-caffeoylquinic acid [55]. A signal demonstrated an [M-H]- $m/z$  at 193 daughter ions at 161, 133, 115, 105, and 77; it was tentatively identified as 3-hydroxy-4-methoxycinnamic acid (isoferulic acid) [56]. A signal demonstrated an [M-H]- $m/z$  at 163 and daughter ions at 119 [M-H-CO<sub>2</sub>]-, and 59; it was tentatively identified as 2-hydroxycinnamic acid (o-coumaric acid) [57]. A signal demonstrated an [M-H]- $m/z$  at 353 and daughter ions at 191 [M-H-caffeic acid moiety]-, 173 [M-H-caffeic acid moiety-H<sub>2</sub>O]-, 135 and 85; it was tentatively identified as 4-O-caffeoylquinic acid [55]. A signal demonstrated an [M-H]- $m/z$  at 515 and daughter ions at 353, 335 [M-H-H<sub>2</sub>O]-, 191 [M-H-

caffeic acid moiety]-, 179 [M-H-quinic acid moiety]-, 161 and 135; it was tentatively identified as 1,3-O-dicaffeoylquinic acid [55] (cynarin). A signal demonstrated an [M-H]- $m/z$  at 183 and daughter ions at 168 [M-H-CH<sub>3</sub>]-, 124 [M-H-CH<sub>3</sub>-CO<sub>2</sub>]-, 93 and 78; it was tentatively identified as methyl gallate [30]. A signal demonstrated an [M-H]- $m/z$  at 515 daughter ions at 353 [M-H-caffeic acid moiety]-, 191 [M-H-2caffeic acid moiety]-, 179 [M-H-caffeic acid moiety-quinic acid moiety]-, and 135; it was tentatively identified as 4,5-dicaffeoylquinic acid [55].

### 3.4.2. Flavonoids

A signal demonstrated an [M-H]- $m/z$  at 609 and daughter ions at 447 [M-H-Glc]-, and 285 447 [M-H-2Glc]-; it was tentatively identified as luteolin-7,3'-di-O-glucoside [53]. A signal demonstrated an [M-H]- $m/z$  at 463 and daughter ions at 335, 301 [M-H-Glc]-, 300, 283 [M-H-Glc-H<sub>2</sub>O]-, 259 and 203; it was tentatively identified as quercetin 3-O-galactoside (hyperoside) [53]. A signal demonstrated an [M-H]- $m/z$  at 593 and daughter ions at 423, and 285 [M-H-Glc-Rha]-; it was tentatively identified as datiscetin 3-O-rutinoside (datiscin) [58]. A signal demonstrated an [M-H]- $m/z$  at 461 and daughter ions at 447, 357, 285 [M-H-GlcA]-, 151 and 113; it was tentatively identified as scutellarein-7-glucuronide (scutellarin) [59]. A signal demonstrated an [M-H]- $m/z$  at 447 and daughter ions at 327, 285 [M-H-glucose moiety]-, 256 217 [luteolin-C<sub>2</sub>H<sub>2</sub>O-C<sub>2</sub>H<sub>2</sub>]-, 199 [luteolin-CHO-2CO-H]-, and 151; it was tentatively identified as luteolin 7-glucoside [51]. A signal demonstrated an [M-H]- $m/z$  at 447 and a daughter ion at 285 [M-H-glucose moiety]-; it was tentatively identified as luteolin-4'-O-glucoside [55]. A signal demonstrated an [M-H]- $m/z$  at 607 daughter ions at 299 [M-H-Glc-Rha]-, and 284 [M-H-Glc-Rha-CH<sub>3</sub>]-; it was tentatively identified as diosmetin 7-O-rutinoside (diosmin) [60]. A signal demonstrated an [M-H]- $m/z$  at 431 daughter ions at 311, 269 [M-H-glucose moiety]-, 151 and 117; it was tentatively identified as apigenin 7-glucoside [55]. A signal demonstrated an [M-H]- $m/z$  at 461 daughter ions at 446 [M-H-CH<sub>3</sub>]-, 313, 299 [M-H-Glc]-, 284 [M-H-Glc-CH<sub>3</sub>]-, and 256 [M-H-Glc-CH<sub>3</sub>-CO]-; it was tentatively identified as tectoridin [61]. A signal demonstrated an [M-H]- $m/z$  at 529 and daughter ions at 428, 367 [M-H-Glc]-, 241, 179, and 149; it was tentatively identified as icaraside [62]. A signal demonstrated an [M-H]- $m/z$  at 285

daughter ions at 241, 199, 175, 151, 133, 107, and 65; it was tentatively identified as 7,8,3',4'-Tetrahydroxyflavone [63]. A signal demonstrated an [M-H]<sup>-</sup>*m/z* at 269 daughter ions at 225, 151, 117, 107, and 65; it was tentatively identified as apigenin [55]. A signal demonstrated an [M-H]<sup>-</sup>*m/z* at 299 daughter ions at 284 [M-H-CH<sub>3</sub>]<sup>-</sup>, 256 [M-H-CH<sub>3</sub>-CO]<sup>-</sup>, 227, and 211; it was tentatively identified as chrysoeriol [64].

### 3.4.3. Coumarins

A signal demonstrated an [M-H]<sup>-</sup>*m/z* at 339 and daughter ions at 177 [M-H-glucose moiety]<sup>-</sup>, and 133; it was tentatively identified as esculin [65]. A signal demonstrated an [M-H]<sup>-</sup>*m/z* at 177 and daughter ions at 149 [M-H-CO]<sup>-</sup>, 133 [M-H-2CO-CO<sub>2</sub>]<sup>-</sup>, 105 [M-H-CO-CO<sub>2</sub>]<sup>-</sup>, 89 and 77; it was tentatively identified as 7,8-dihydroxycoumarin (daphnetin) [66].

### 3.4.4. Anthraquinones

A signal demonstrated an [M-H]<sup>-</sup>*m/z* at 415 and daughter ions at 269 [M-H-Rha]<sup>-</sup>, 161, and 101; it was tentatively identified as frangulin A [67].

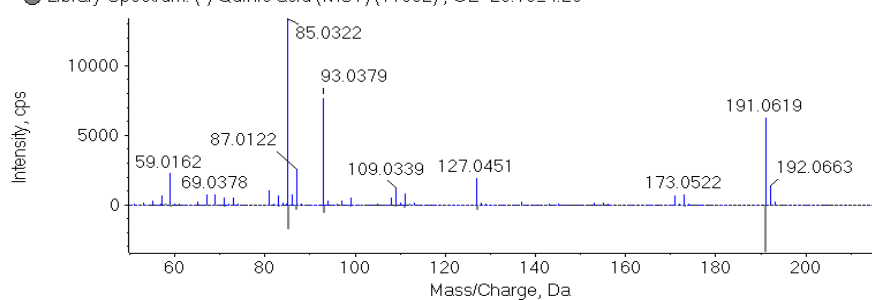
### 3.4.5. Others

A signal demonstrated an [M-H]<sup>-</sup>*m/z* at 109 and daughter ions at 108, 91 [M-H-H<sub>2</sub>O]<sup>-</sup>, 65, and 53; it was tentatively identified as pyrocatechol [68]. A signal demonstrated an [M-H]<sup>-</sup>*m/z* at 137 and daughter ions at 119 [M-H-H<sub>2</sub>O]<sup>-</sup>, 109 [M-H-CO]<sup>-</sup>, 108, 81, 65, and 53; it was tentatively identified as 3,4-dihydroxybenzaldehyde (protocatechuic aldehyde) [69]. A signal demonstrated an [M-H]<sup>-</sup>*m/z* at 121 daughter ions at 108, 93 [M-H-CO]<sup>-</sup>, 92 and 65; it was tentatively identified as 3-hydroxybenzaldehyde [70].

Table 4: Chemical constituents of *D. carota* leaf extract.

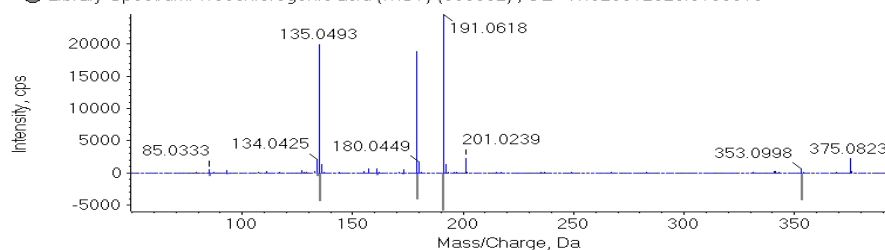
No.	Rt	[M-H] <sup>-</sup>	M.wt.	M.F.	Identified compound	Chemical class
1	2.92	191	192	C <sub>7</sub> H <sub>12</sub> O <sub>6</sub>	Quinic acid	Carboxylic acids
2	3.11	133	134	C <sub>4</sub> H <sub>6</sub> O <sub>5</sub>	Malic acid	Carboxylic acids
3	3.14	115	116	C <sub>4</sub> H <sub>4</sub> O <sub>4</sub>	Maleic acid	Carboxylic acids
4	10.18	137	138	C <sub>7</sub> H <sub>6</sub> O <sub>3</sub>	3-Hydroxybenzoic acid	Phenolic acids
5	10.64	167	168	C <sub>8</sub> H <sub>8</sub> O <sub>4</sub>	Vanillic acid	Phenolic acids
6	11.06	179	180	C <sub>9</sub> H <sub>8</sub> O <sub>4</sub>	Caffeic acid	Phenolic acids
7	11.12	353	354	C <sub>16</sub> H <sub>18</sub> O <sub>9</sub>	Neochlorogenic acid	Phenolic acids
8	11.16	515	516	C <sub>25</sub> H <sub>24</sub> O <sub>12</sub>	1,5-Dicaffeoylquinic acid	Phenolic acids
9	10.92	515	516	C <sub>25</sub> H <sub>24</sub> O <sub>12</sub>	3,5-Di-O-caffeoylquinic acid	Phenolic acids
10	11.22	109	110	C <sub>6</sub> H <sub>6</sub> O <sub>2</sub>	Pyrocatechol	Benzene derivatives
11	11.34	339	340	C <sub>15</sub> H <sub>16</sub> O <sub>9</sub>	Esculin	Coumarins
12	11.40	193	194	C <sub>10</sub> H <sub>10</sub> O <sub>4</sub>	Isoferulic acid	Phenolic acids
13	11.62	163	164	C <sub>9</sub> H <sub>8</sub> O <sub>3</sub>	o-Coumaric acid	Phenolic acids
14	11.70	353	354	C <sub>16</sub> H <sub>18</sub> O <sub>9</sub>	4-O-Caffeoylquinic acid	Phenolic acids
15	11.91	415	416	C <sub>21</sub> H <sub>20</sub> O <sub>9</sub>	Frangulin A	Anthraquinones
16	12.10	515	516	C <sub>25</sub> H <sub>24</sub> O <sub>12</sub>	1,3-O-dicaffeoylquinic acid (Cynarin)	Phenolic acids
17	12.12	609	610	C <sub>27</sub> H <sub>30</sub> O <sub>16</sub>	Luteolin-7,3'-di-O-glucoside	Flavonoids
18	12.14	137	138	C <sub>7</sub> H <sub>6</sub> O <sub>3</sub>	Protocatechuic aldehyde	Benzaldehydes
19	12.20	183	184	C <sub>8</sub> H <sub>8</sub> O <sub>5</sub>	Methyl gallate	Phenolic esters
20	12.30	463	464	C <sub>21</sub> H <sub>20</sub> O <sub>12</sub>	Quercetin 3-O-galactoside (Hyperoside)	Flavonoids
21	12.48	593	594	C <sub>27</sub> H <sub>30</sub> O <sub>15</sub>	Datisetin 3-O-rutinoside (Datiscin)	Flavonoids
22	12.51	177	178	C <sub>9</sub> H <sub>6</sub> O <sub>4</sub>	7,8-Dihydroxycoumarin(Daphnetin)	Coumarins
23	12.81	461	462	C <sub>21</sub> H <sub>18</sub> O <sub>12</sub>	Scutellarin	Flavonoids
24	12.83	447	448	C <sub>21</sub> H <sub>20</sub> O <sub>11</sub>	Luteolin 7-glucoside	Flavonoids
25	12.84	447	448	C <sub>21</sub> H <sub>20</sub> O <sub>11</sub>	Luteolin-4'-O-glucoside	Flavonoids
26	12.99	607	608	C <sub>28</sub> H <sub>32</sub> O <sub>15</sub>	Diosmin	Flavonoids
27	13.34	121	122	C <sub>7</sub> H <sub>6</sub> O <sub>2</sub>	3-Hydroxybenzaldehyde	Hydroxybenzaldehydes
28	13.36	431	432	C <sub>21</sub> H <sub>20</sub> O <sub>10</sub>	Apigenin 7-glucoside	Flavonoids
29	13.42	461	462	C <sub>22</sub> H <sub>22</sub> O <sub>11</sub>	Tectoridin	Flavonoids
30	13.47	515	516	C <sub>25</sub> H <sub>24</sub> O <sub>12</sub>	4,5-Dicaffeoylquinic acid	Phenolic acids
31	14.30	529	530	C <sub>27</sub> H <sub>30</sub> O <sub>10</sub>	Icariside	Flavonoids
32	14.97	285	286	C <sub>15</sub> H <sub>10</sub> O <sub>6</sub>	7,8,3',4'-Tetrahydroxyflavone	Flavonoids
33	15.84	269	270	C <sub>15</sub> H <sub>10</sub> O <sub>5</sub>	Apigenin	Flavonoids
34	16.03	299	300	C <sub>16</sub> H <sub>12</sub> O <sub>6</sub>	Chrysoeriol	Flavonoids

■ Spectrum from CHE\_231\_November-2022-Negativ...-200] (50 - 1000) from 3.032 to 3.254 min]  
● Library Spectrum: (-)-Quinic acid (NIST) (77952) , CE=25.75±4.25



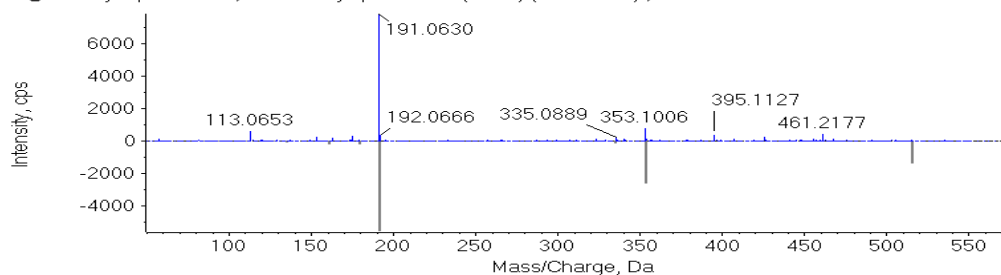
### Quinic acid

■ Spectrum from CHE\_231\_November-2022-Negativ...00] (50 - 1000) from 11.127 to 11.289 min]  
● Library Spectrum: Neochlorogenic acid (NIST) (906332) , CE=47.3203125±8.6796875



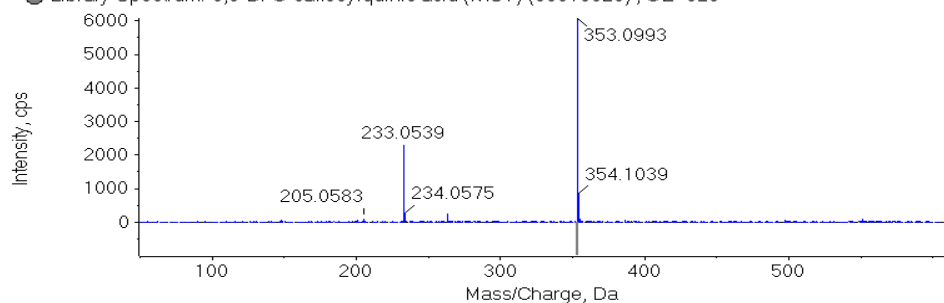
### Neochlorogenic acid

■ Spectrum from CHE\_231\_November-2022-Negativ...50] (50 - 1000) from 11.303 to 11.586 min]  
● Library Spectrum: 1,5-Dicaffeoylquinic acid (NIST) (19870463) , CE=47.1640625±8.8359375

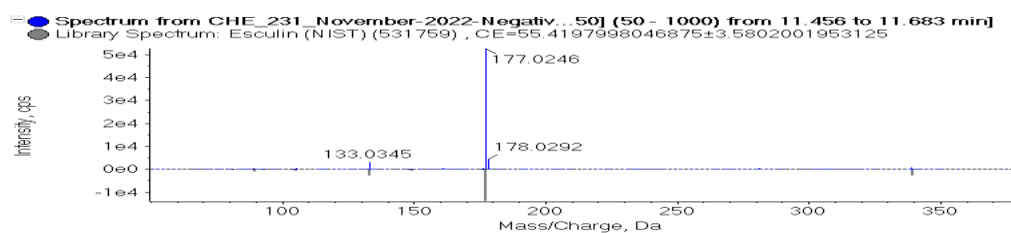
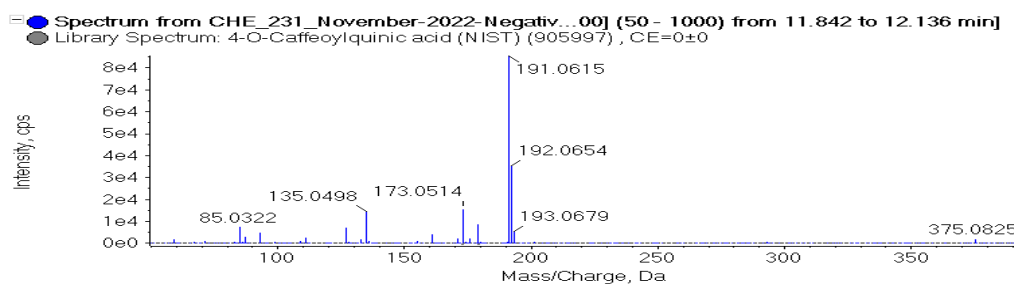
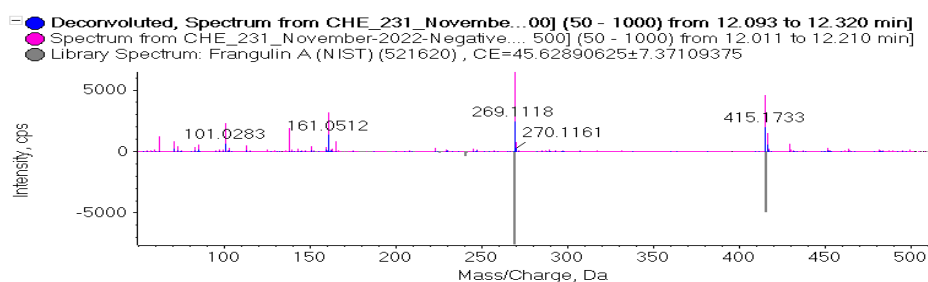
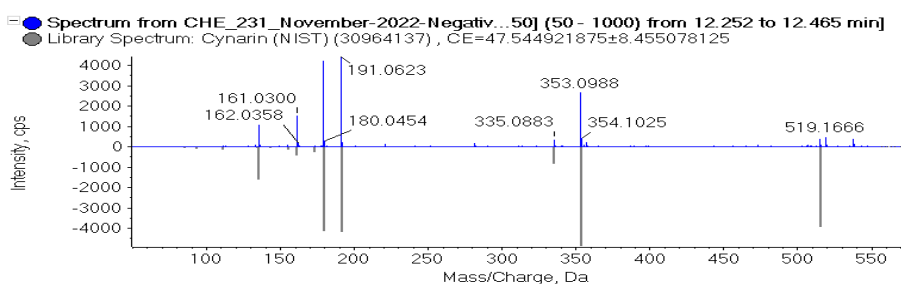
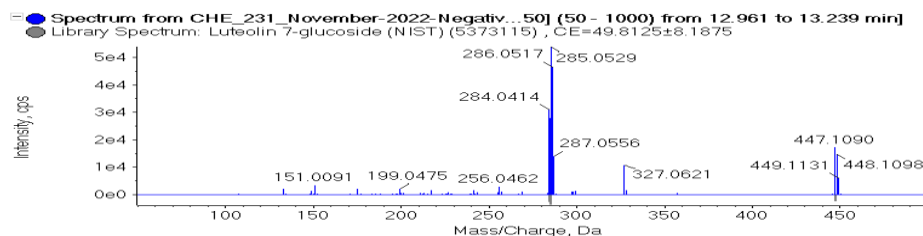


### 1,5-Dicaffeoylquinic acid

■ Spectrum from CHE\_231\_November-2022-Negativ...00] (50 - 1000) from 11.041 to 11.277 min]  
● Library Spectrum: 3,5-Di-O-caffeoylquinic acid (NIST) (89919620) , CE=0±0



### 3,5-Di-O-caffeoylquinic acid

**Esculin****4-O-Caffeoylquinic acid****Frangulin A****Cynarin****Luteolin 7-glucoside**Fig. 1. MS/MS spectra of some identified compounds in *D. carota* leaf extract.

### 3.5.1. Virtual Screening-based Target Identification

In order to figure out how the *D. carota* leaf extract exerts its antibacterial activity, particularly against *S. aureus* and *E. coli*, all the modeled structures of the LC-MS-annotated compounds were subjected to pharmacophore-based virtual screening using PharmMapper platform<sup>[22]</sup>. PharmMapper can screen and suggest the most likely protein targets of a query molecule based on its pharmacophore model by mapping its key pharmacophore features (i.e., spatial arrangement of structural features).

Accordingly, molecules that conform to these pharmacophore maps have a greater potential for binding to the same protein targets. Therefore, the annotated compounds in the *D. carota* leaf extract were run through PharmMapper to find the potential protein target(s). The results that were retrieved were ranked by how well they fit the criteria (i.e., Fit score). Only bacterial targets that were selected, particularly those relevant to the *S. aureus* and *E. coli*.

As a result, Pyruvate Kinase (PyK) of *S. aureus* and *E. coli* (PDB ID: 3T0T and 1PKY, respectively) were found to be the top-scoring hits for caffeic acid, isoferulic acid, and apigenin (Fit scores = 12.41, 10.64, and 5.87, for *S. aureus* PyK; 11.16, 10.53, and 5.66 for *E. coli* PyK, respectively; Figure 2), and hence, these metabolites in *D. carota* leaf extract can be considered putatively as the key bioactive compounds that mediate its antibacterial activity.

It is well-known that PK is an essential protein catalyzing the last step of glycolysis, in which a phosphoryl group is transferred from phosphoenolpyruvate to ADP, leading to the formation of pyruvate and ATP. Accordingly, PyK has been found to be a key antibacterial target that can be utilized for the development of new generation of antibiotics<sup>[71, 72]</sup>.

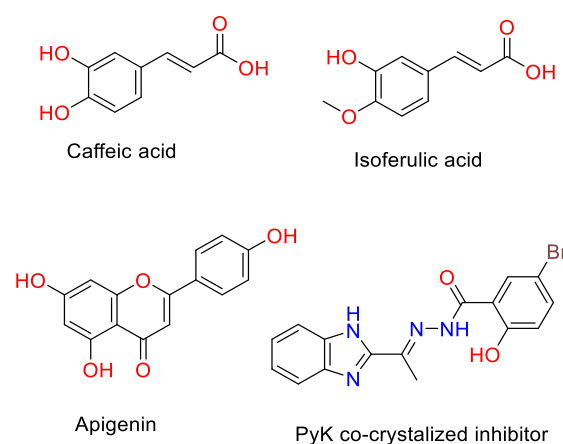


Fig. 2. Structures that were found to be probably able to bind with *S. aureus* and *E. coli* PyK according to the preliminary PharmMapper-based virtual screening alongside the PyK co-crystallized inhibitor.

### 3.5.2. Molecular docking and dynamics simulation analysis

In order to investigate the binding modes of each aforementioned compound (Figure 2) with PyK of both *S. aureus* and *E. coli*, their modeled structures were prepared and re-docked into the active sites of each protein. Subsequently, the retrieved binding poses were subjected to 50 ns-long MD simulation runs to validate the binding stability affinity of each compound inside the active sites of the suggested protein targets. First, re-docking of each structure into the PyK's active site achieved binding modes and docking scores comparable to those of the co-crystallized inhibitor (Figures 3-5 and Table 5).

As shown in Figures 3A, 3B, and 3D, caffeic acid and iso-ferulic acid were able to achieve binding modes quite similar to that of the co-crystallized inhibitor forming also similar hydrophilic and hydrophobic interactions (Table 5). The key differences were the electrostatic interactions between the carboxylic group of both compounds and HIS-365B (in case of *S. aureus* PyK) and ARG-360B (in case of *E. coli* PyK).

In regard to apigenin (Figure 3C), it showed a binding mode comparable to that of caffeic and iso-ferulic acids, however it formed only a single H-bond with SER-362A in case of *S. aureus* PyK, and ARG-360A in case of *E. coli* PyK.

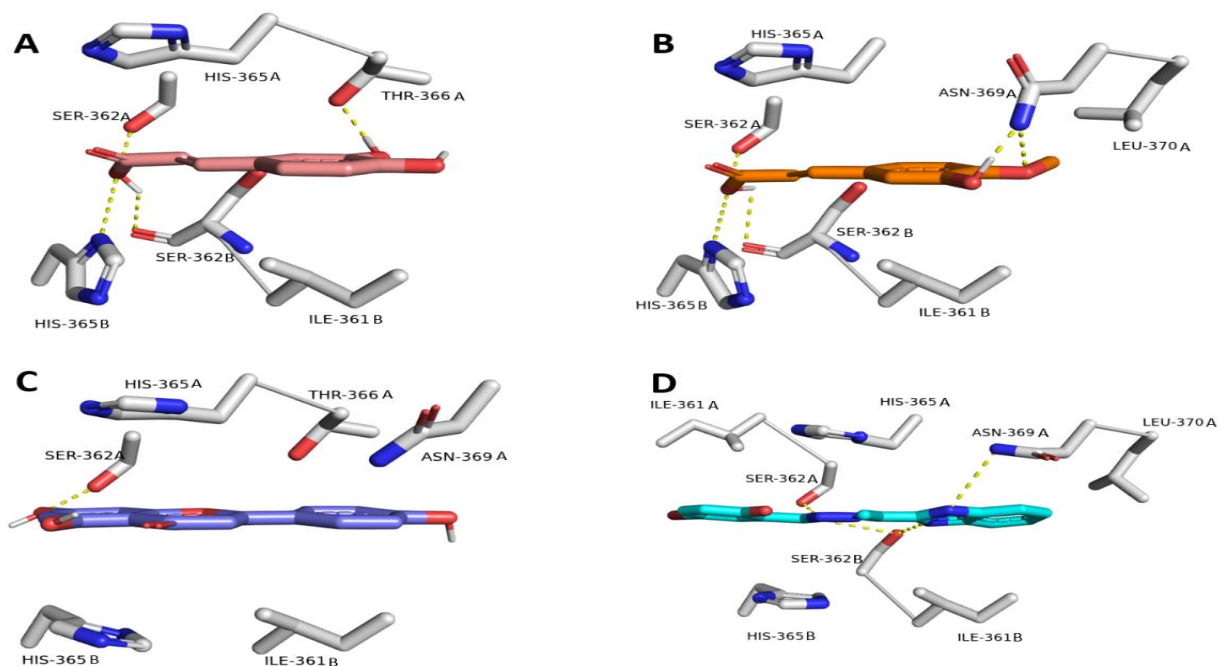


Fig. 3. Binding modes of caffeic acid (brick red-colored structure), iso-ferulic acid (orange-colored structure), and apigenin (blue-colored structure) along with the co-crystallized inhibitor (Cyan-colored structure) inside the binding site of PyK of *S. aureus* (PDB ID: 3T0T).

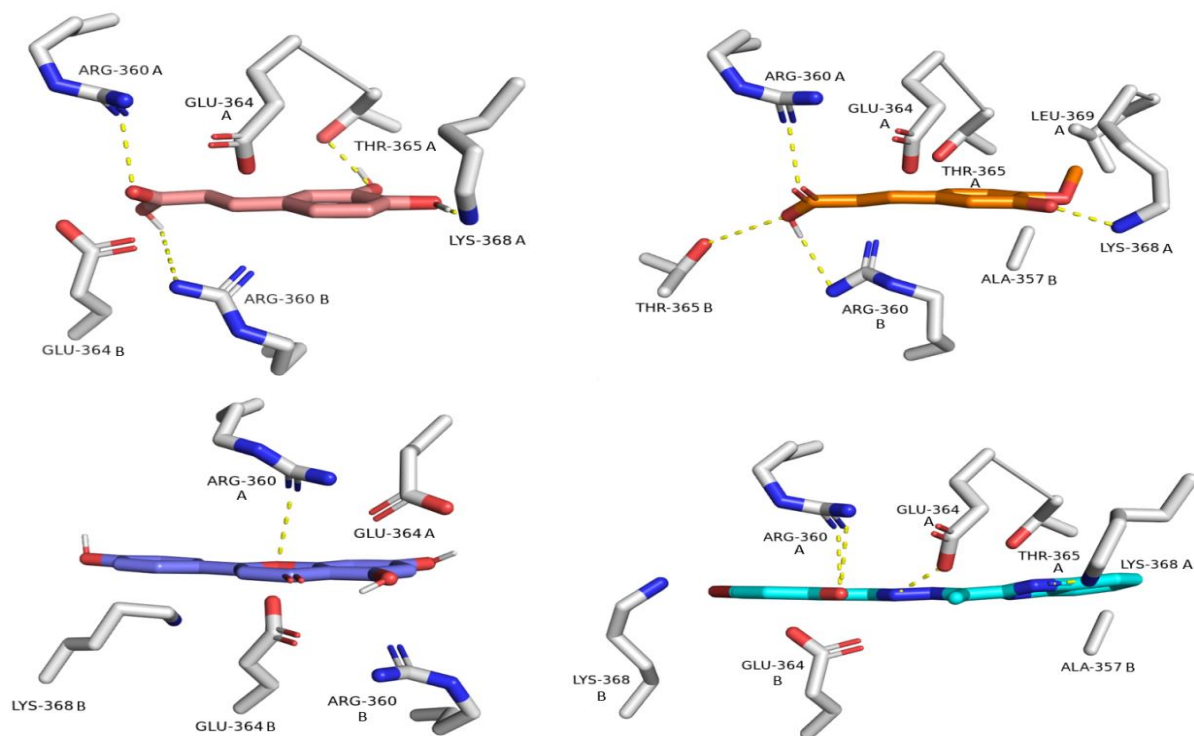


Fig. 4. Binding modes of caffeic acid (brick red-colored structure), iso-ferulic acid (orange-colored structure), and apigenin (blue-colored structure) along with the co-crystallized inhibitor (Cyan-colored structure) inside the binding site of PyK of *E. coli* (PDB ID: 1PKY).

Table 5: Docking scores and  $\Delta G_{\text{Bind}}$  (in kcal/mol) of caffeic acid, isoferulic acid, and apigenin inside *S. aureus* and *E. coli* PyK's active sites.

Compound	Docking score		MM-PBSA ( $\Delta G_{\text{Bind}}$ )		H-Bonds		Hydrophobic interactions	
	PyK <sub>St</sub>	PyK <sub>col</sub>	PyK <sub>St</sub>	PyK <sub>col</sub>	PyK <sub>St</sub>	PyK <sub>col</sub>	PyK <sub>St</sub>	PyK <sub>col</sub>
Caffeic acid	-12.87	-12.23	-	-9.58	SER- 362A,B; THR-366A; HIS-365B	ARG- 360A,B; THR- 365A	ILE-361B	-
Iso-ferulic acid	-12.35	-12.11	-	-10.44	SER- 362A,B; ASN-369A; HIS-365B	ARG- 360A,B; THR- 365B; LYS- 368A	ILE- 361B; LEU- 370A	LEU-369A
Apigenin	-7.98	-7.46	-2.13	-1.955	SER-362A	ARG- 360A	ILE-361B	LYS-368B
Co-crystallized inhibitor	-10.44	-10.28	-8.48	-8.13	SER- 362A,B; ASN-369A	ARG- 360A; GLU- 364A; THR- 365A	ILE- 361A,B; LEU- 370A	LYS-368A

Subsequent molecular dynamic (MD) simulation experiments (50 ns-long) revealed that both caffeic and iso-ferulic acids were able to achieve stable binding modes over the course of simulation with an average RMSD of  $\sim 1.9$  Å and  $\sim 2.1$  Å inside the PyK's active sites of *S. aureus* and *E. coli* (Figure 3A and 3B, respectively) that were also comparable to that of the co-crystallized inhibitor (average RMSD  $\sim 1.5$  Å and  $1.6$  Å for respectively).

Such stable bindings of both caffeic and iso-ferulic acids were translated into very good affinities (expressed as  $\Delta G_{\text{Bind}}$ ) toward each

enzyme that was convergent to that of the co-crystallized inhibitor (Table 5).

According to the previous modeling and MD simulation findings, it can be concluded that caffeic and iso-ferulic acids are likely able to inhibit the growth of *S. aureus* and *E. coli* via targeting their PyK.

Several previous reports have illustrated the antibacterial potential of caffeic acid and its derivatives, particularly against *S. aureus* and *E. coli* indicating that this interesting scaffold is capable of fighting these two pathogenic bacteria via multiple mechanisms<sup>[73-75]</sup>.

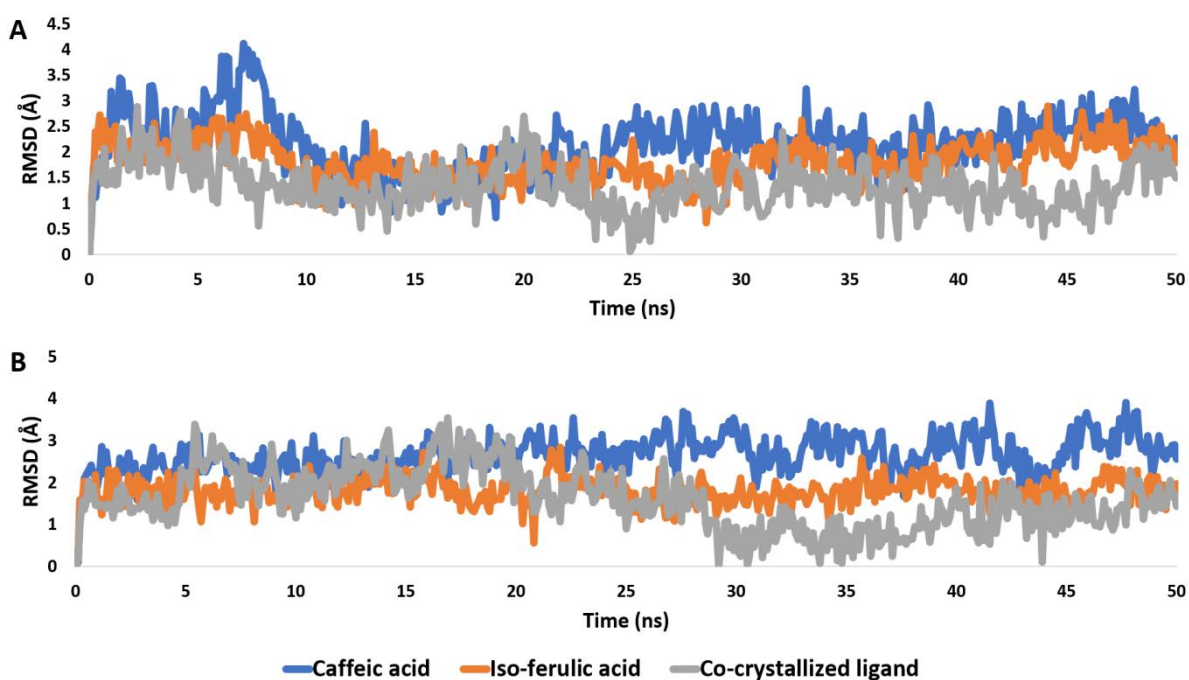


Fig. 5. RMSDs of both caffeic and iso-ferulic acids inside the PyK binding sites of *S. aureus* and *E. coli* over the course of 50 ns-long MD simulation.

#### 4. Conclusion

The present study annotated 34 compounds from the *D. carota* leaf extract via UPLC-QTOF-MS/MS. It also suggested *D. carota* as a promising source of naturally occurring antioxidant and antimicrobial agents. The comprehensive virtual screening and MD simulation study of the annotated compounds highlighted both caffeic and iso-ferulic acids as probable new antibacterial agents acting by unusual mode action (i.e., inhibition of PyK). Further investigations can be performed on the

chromatographic isolation and structure elucidation of the desired ingredients as promising leads for therapeutic applications.

#### Abbreviations

UPLC-QTOF/MS: Ultra-high performance liquid chromatography-quadrupole time-of-flight mass spectrometry; TPC: Total phenolic content; TAC: Total antioxidant capacity; GAE: Gallic acid equivalent; MTP: Microtiter plate assay; MDS: Molecular dynamics simulation; PyK: Pyruvate kinase.

#### Acknowledgments

The authors would like to thank the Academy of Scientific Research and Technology (ASRT), Cairo, Egypt; Theodor Bilharz Research Institute (TBRI), Giza, Egypt; and Ain Shams University (ASU), Cairo, Egypt for technical and financial support.

#### Finding

The study is funded by the Academy of Scientific Research and Technology (Scientists for Next Generation Scholarship).

#### Conflict of interest

No potential conflicts of interest were reported by the authors.

#### References

1. Glisic SB, Mistic DR, Stamenic MD, Zizovic IT, Asanin RM, Skala DU. Supercritical carbon dioxide extraction of carrot fruit essential oil: Chemical composition and antimicrobial activity. *Food Chem* 2007; 105: 346-352.
2. Jabrane A, Jannet HB, Harzallah-Skhiri F, Mastouri M, Casanova J, Mighri Z. Flower and root oils of the Tunisian *Daucus carota* L. ssp. *maritimus*(Apiaceae): integrated analyses by GC, GC/MS, and  $^{13}\text{C}$ -NMR spectroscopy, and

- in vitro* antibacterial activity. *ChemBiodivers* 2009; 6: 881-889.
- Majdouba S, El Moknib R, Muradalieviche AA, Pirasg A, Porceddag S, Hammamia S. Effect of pressure variation on the efficiency of supercritical fluid extraction of wild carrot (*Daucus carota* subsp. *maritimus*) extracts. *J Chromatogr B* 2019; 1125: 121713.
  - Ahmed AA, Bishr MM, El-Shanawany MA, Attia EZ, Ross SA, Pare PW. Rare trisubstituted sesquiterpenes daucanes from the wild *Daucus carota*. *Phytochemistry* 2005; 66: 1680-1684.
  - Kumarasamy Y, Nahar L, Byres M, Delazar A, Sarker SD. The assessment of biological activities associated with the major constituents of the methanol extract of wild carrot (*Daucus carota* L.) seeds. *J Herb Pharmacother* 2005; 5: 61-72.
  - Stojanovic Z, Dor N, Radulovic N. Volatiles of the Balkan endemic *Daucus guttatus* ssp. *zahariadii* and cultivated and wild-growing *D. carota* - a comparison study. *Food Chem* 2011; 125: 35-43.
  - Shebaby WN, El-sibai M, Smith KB, Karam MC, Mroueh M, Daher CF. The antioxidant and anticancer effects of wild carrot oil extract. *Phytother Res* 2013; 27: 737-744.
  - Cosimi E, Cioni PL, Molfetta I, Braca A. Essential-oil composition of *Daucus carota* ssp. *major* (Pastinocellocarrot) and nine different commercial varieties of *Daucus carota* ssp. *sativus* fruits. *ChemBiodivers* 2014; 11: 1022-1033.
  - Sivanantham S, Thangaraj N. Phytochemical screening, characterization, compound identification and separation from *Daucus carota* L. *Int J Curr Res Biosci Plant Biol* 2015; 2(7): 168-172.
  - Ghareeb MA, Ahmed WS, Refahy LA, Abdou AM, Hamed MM, Abdel-Aziz MS. Isolation and characterization of the bioactive phenolic compounds from *Morus alba* L. growing in Egypt. *Pharmacologyonline* 2016; 3: 157-167.
  - Caicedo C, Iuga C, Castañeda-Arriagaa R, Alvarez-Idaboy JR. Antioxidant activity of selected natural polyphenolic compounds from soybean via peroxy radical scavenging. *RSC Adv* 2014; 4: 38918.
  - Lobo V, Patil A, Phatak A, Chandra N. Free radicals, antioxidants and functional foods: Impact on human health. *Pharmacogn Rev* 2010; 4(8): 118-126.
  - Álvarez-Martínez FJ, Barrajón-Catalán E, Micol V. Tackling antibiotic resistance with compounds of natural Origin: A comprehensive review. *Biomedicine* 2020; 8(10): 405.
  - Borges A, Saavedra MJ, Simões M. Insights on antimicrobial resistance, biofilms and the use of phytochemicals as new antimicrobial agents. *Curr Med Chem* 2015; 22(21): 2590-2614.
  - Mishra R, Panda AK, De Mandal S, Shakeel M, Bisht SS, Khan J. Natural anti-biofilm agents: Strategies to control biofilm-forming pathogens. *Front Microbiol* 2020; 11: 566325.
  - Shirwaikar A, Rajendran K, Punithaa IS. *In vitro* antioxidant studies on the benzyl tetra isoquinoline alkaloid berberine. *Biol Pharm Bull* 2006; 29(9): 1906-1910.
  - Prieto P, Pineda M, Aguilar M. Spectrophotometric quantation of antioxidant capacity through the formation of a phosphomolybdenum complex: Specific application to the determination of vitamin E. *Anal Biochem* 1999; 269: 337-341.
  - Kumar KS, Ganesan K, Rao PV. Antioxidant potential of solvent extracts of *Kappaphycus alvarezii* (Doty). Edible seaweed. *Food Chem* 2008; 107: 289-295.
  - Elkhouly HI, Hamed AA, El Hosainy AM, Ghareeb MA, Sidkey NM. Bioactive secondary metabolite from endophytic *Aspergillus Tubenginses* ASH4 isolated from *Hyoscyamus muticus*: Antimicrobial, antibiofilm, antioxidant and anticancer activity. *Pharmacogn J* 2021a; 13(2): 434-442.
  - Elkhouly HI, Sidkey NM, Ghareeb MA, El Hosainy AM, Hamed AA. Bioactive Secondary Metabolites from Endophytic *Aspergillus terreus* AH1 Isolated from *Ipomoea carnea* Growing in Egypt. *Egypt J Chem* 2021b; 64(12): 7511-7520.
  - El-Shazly MAM, Hamed AA, Kabary HA, Ghareeb MA. LC-MS/MS profiling, antibiofilm, antimicrobial and bacterial growth kinetic studies of *Pluchea dioscoridis* extracts. *Acta Chromatogr* 2022; 34(3): 338-350.
  - Wang X, Shen Y, Wang S, Li S, Zhang W, Liu X, Lai L, Pei J, Li H. PharmMapper 2017 update: A web server for potential drug target identification with a comprehensive target pharmacophore database. *Nucleic Acids Res* 2017; 45: W356-W360.
  - Huey R, Morris GM, Forli S. Using AutoDock 4 and AutoDock vina with AutoDockTools: a tutorial. *The Scripps Research Institute Molecular Graphics Laboratory*, 10550(92037), 1000, 2012.
  - Yuan S, Chan HS, Hu Z. Using PyMOL as a platform for computational drug design. *Wiley Interdiscip Rev Comput Mol Sci* 2017; 7(2): e1298.
  - Phillips JC, Braun R, Wang W, Gumbart J, Tajkhorshid E, Villa E, Chipot C, Skeel RD,

- Kalé L, Schulten K. Scalable molecular dynamics with NAMD. *J Comput Chem* 2005; 26: 1781-1802.
26. Ribeiro JV, Bernardi RC, Rudack T, Schulten K, Tajkhorshid E. QwikMD-Gateway for Easy Simulation with VMD and NAMD. *Biophys J* 2018; 114(3): 673a-674a.
27. Humphrey W, Dalke A, Schulten K. VMD: visual molecular dynamics. *J Mol Graph* 1996; 14(1): 33-38.
28. Miller III BR, McGee Jr TD, Swails JM, Homeyer N, Gohlke H, Roitberg AE. MMPBSA.py: an efficient program for end-state free energy calculations. *J Chem Theory Comput* 2012; 8: 3314-3321.
29. Ghareeb M, Sobeh M, Rezaq S, El-Shazly A, Mahmoud M, Wink M. HPLC-ESI-MS/MS profiling of polyphenolics of a leaf extract from *Alpinia zerumbet* (Zingiberaceae) and its anti-inflammatory, anti-nociceptive, and antipyretic activities *in vivo*. *Molecules* 2018a; 23(12): 3238.
30. Ghareeb MA, Mohamed T, Saad AM, Refahy LA, Sobeh M, Wink M. HPLC-DAD-ESI-MS/MS analysis of fruits from *Firmiana simplex* (L.) and evaluation of their antioxidant and antigenotoxic properties. *J Pharm Pharmacol* 2018b; 70: 133-142.
31. Ghareeb M, Saad A, Ahmed W, Refahy L, Nasr S. HPLC-DAD-ESI-MS/MS characterization of bioactive secondary metabolites from *Strelitzia nicolai* leaf extracts and their antioxidant and anticancer activities *in vitro*. *Pharmacogn Res* 2018c; 10: 368.
32. Sobeh M, Mahmoud MF, Hasan RA, Abdelfattah MAO, Sabry OM, Ghareeb MA, El-Shazly AM, Wink M. Tannin-rich extracts from *Lannea stuhlmannii* and *Lannea humilis* (Anacardiaceae) exhibit hepatoprotective activities *in vivo* via enhancement of the anti-apoptotic protein Bcl-2. *Sci Rep* 2018; 8: 9343.
33. Ayeni EA, Ahmed A, Ibrahim G, Vallada A, Muhammad ZH. Phytochemical, nutraceutical and antioxidant studies of the aerial parts of *Daucus carota* L. (Apiaceae). *J Herbm Pharm* 2018; 7(2): 68-73.
34. Rice-Evans CA, Miller NJ, Paganga G. Structure-antioxidant activity relationships of flavonoids and phenolic acids. *Free Radic Biol Med* 1996; 20(7): 933-956.
35. Soobrattee MA, Neergheen VS, Luximon-Ramma A, Aruoma OI, Bahorun T. Phenolics as potential antioxidant therapeutic agents: Mechanism and actions. *Mutat Res* 2005; 579: 200-213.
36. Chen J, Yang J, Ma L, Li J, Shahzad N, Kim CK. Structure-antioxidant activity relationship of methoxy, phenolic hydroxyl, and carboxylic acid groups of phenolic acids. *Sci Rep* 2020; 10: 2611.
37. Ghareeb MA, Refahy LA, Saad AM, Osman NS, Abdel-Aziz MS, El-Shazly MA, Mohamed AS. *In vitro* antimicrobial activity of five Egyptian plant species. *J Appl Pharm Sci* 2015; 5: 045-049.
38. Saad AM, Mohammed MMD, Ghareeb MA, Ahmed WS, Farid MA. Chemical composition and antimicrobial activity of the essential oil of the leaves of *Cupressus macrocarpa* Hartweg. *J Appl Pharm Sci* 2017; 7: 207-212.
39. Mohammed HS, Abdel-Aziz MM, Abubaker MS, Saad AM, Mohamed MA, Ghareeb MA. **Antibacterial and potential antidiabetic activities of flavone C-glycosides isolated from *Beta vulgaris* subspecies *cicla* L. var. *flavescens* (Amaranthaceae) cultivated in Egypt.** *Curr Pharm Biotechnol* 2019; 20(7): 595-604.
40. Khalaf OM, Abdel-Aziz MS, El-Hagrassi AM, Osman AF, Ghareeb MA. Biochemical aspect, antimicrobial and antioxidant activities of *Melaleuca* and *Syzygium* species (Myrtaceae) grown in Egypt. *J PhysConfSer* 2021; 1879: 022062.
41. Shafik NH, Shafek RE, Michael HN. Antimicrobial activity of different extracts of *Daucus carota* canopy. *Int J Pharm* 2015; 5(2):352-356.
42. Cowan MM. Plant products as antimicrobial agents. *Clin Microb Rev* 1999; 12(4): 564-582.
43. Tim Cushman TP, Lamb AJ. Antimicrobial activity of flavonoids. *Int J Antimicrob Agents* 2005; 26: 343-356.
44. Shamsudin NF, Ahmed QU, Mahmood S, Ali Shah SA, Khatib A, Mukhtar S, Alsharif MA, Parveen H, Zakaria ZA. Antibacterial effects of flavonoids and their structure-activity relationship study: A comparative interpretation. *Molecules* 2022; 27: 1149.
45. Gonçalves ASC, Leitão MM, Simões M, Borges A. The action of phytochemicals in biofilm control. *Nat Prod Rep* 2023; 40: 595.
46. Ghareeb MA, Sobeh M, El-Maadawy WH, Mohammed HS, Khalil H, Botros SS, Wink M. Chemical profiling of polyphenolics in *Eucalyptus globulus* and evaluation of its hepato-renal protective potential against cyclophosphamide induced toxicity in mice. *Antioxidants* 2019; 8(9): 415.
47. Ghareeb MA, Sobeh M, Aboushousha T, Esmat M, Mohammed HS, El-Wakil ES. Polyphenolic profile of *Herniaria hemistemon* aerial parts extract and assessment of its anti-cryptosporidiosis in a murine model: *In silico*

- supported *in vivo* study. *Pharmaceutics* 2023; 15: 415.
48. Okasha H, Aboushousha T, Coimbra MA, Cardoso SM, Ghareeb MA. Metabolite profiling of *Alocasia gigantea* leaf extract and its potential anticancer effect through autophagy in hepatocellular carcinoma. *Molecules* 2022; 27: 8504.
49. Sayed AM, El-Hawary SS, Abdelmohsen UR, Ghareeb MA. Antiproliferative potential of *Physalis peruviana*-derived magnolin against pancreatic cancer: a comprehensive *in vitro* and *in silico* study. *Food Funct* 2022; 13: 11733.
50. Allen F, Greiner R, Wishart D. Competitive fragmentation modeling of ESI-MS/MS spectra for putative metabolite identification. *Metabolomics* 2015; 11(1): 98-110.
51. Ammar S, Abidi J, Luca SV, Boumendjel M, Skalicka-Woźniak K, Bouaziz M. Untargeted metabolite profiling and phytochemical analysis based on RP-HPLC-DAD-QTOF-MS and MS/MS for discovering new bioactive compounds in *Rumex algeriensis* flowers and stems *Phytochem Anal* 2020; 31: 616-635.
52. Sanz M, de Simón BF, Cadahía E, Esteruelas E, Muñoz AM, Hernández T, Estrella I, Pinto E. LC-DAD/ESI-MS/MS study of phenolic compounds in ash (*Fraxinus excelsior* L. and *F. americana* L.) heartwood. Effect of toasting intensity at cooperage. *J Mass Spectrom* 2012; 47: 905-918.
53. Elessawy FM, Bazghaleh N, Vandenberg A, Purves RW. Polyphenol profile comparisons of seed coats of five pulse crops using a semi-quantitative liquid chromatography-mass spectrometric method. *Phytochem Anal* 2020; 31: 458-471.
54. Cao D, Wang Q, Jin J, Qiu M, Zhou L, Zhou X, Li H, Zhao Z. Simultaneous qualitative and quantitative analyses of triterpenoids in *Ilex pubescens* by ultra-high-performance liquid chromatography coupled with quadrupole time-of-flight mass spectrometry. *Phytochem Anal* 2018; 29: 168-179.
55. Milutinović V, Niketić M, Ušjak L, Nikolić D, Krunic A, Zidorn C, Petrović S. Methanol extracts of 28 *Hieracium* species from the Balkan Peninsula-comparative LC-MS analysis, chemosystematic evaluation of their flavonoid and phenolic acid profiles and antioxidant potentials. *Phytochem Anal* 2018; 29: 30-47.
56. Peng D, Zahid HF, Ajlouni S, Dunshea FR, Suleria HAR. LC-ESI-QTOF/MS profiling of Australian mango peel by-product polyphenols and their potential antioxidant activities. *Processes* 2019; 7: 764.
57. Chanda J, Mukherjee PK, Biswas R, Biswas S, Tiwari AK, Pargaonkar A. UPLC-QTOF-MS analysis of a carbonic anhydrase-inhibiting extract and fractions of *Luffa acutangula* (L.) Roxb (ridge gourd). *Phytochem Anal* 2019; 30: 148-155.
58. Shehata MG, Awad TS, Asker D, El Sohaimey SA, Abd El-Aziz NM Youssef MM. Antioxidant and antimicrobial activities and UPLC-ESI-MS/MS polyphenolic profile of sweet orange peel extracts. *Curr Res Food Sci* 2021; 4: 326-335.
59. Li S, Lin Z, Jiang H, Tong L, Wang H, Chen S. Rapid Identification and assignment of the active ingredients in FufangBanbianlian injection using HPLC-DAD-ESI-IT-TOF-MS. *J Chromatogr Sci* 2016; 54(7): 1225-1237.
60. Zheng Y, Zeng X, Peng W, Wu Z, Su W. Characterisation and classification of *CitriReticulataePericarpium* varieties based on UHPLC-Q-TOF-MS/MS combined with multivariate statistical analyses. *Phytochem Anal* 2019; 30: 278-291.
61. Chen Y, Song W, Peng ZH, Ge BY, Han FM. Identification of metabolites of tectoridin *in-vivo* and *in-vitro* by liquid chromatography-tandem mass spectrometry. *J Pharm Pharmacol* 2008; 60: 709-716.
62. Sun E, Xu F, Qian Q, Cui L, Tan X, Jia X. Ultra-performance liquid chromatography/quadrupole-time-of-flight mass spectrometry analysis of icariside II metabolites in rats. *Nat Prod Res* 2014; 28(19): 1525-1529.
63. Thammarat P, Jiaranaikulwanitch J, Phongpradist R, Raiwa A, Pandith H, Sawangrat K, Sirilun S. Cosmeceutical potentials of *Equisetum debile* Roxb. Extracts. *Appl Sci* 2023; 13: 1336.
64. Aghakhani F, Kharazian N, Gooini ZL. Flavonoid constituents of *Phlomis* (Lamiaceae) species using liquid chromatography mass spectrometry. *Phytochem Anal* 2018; 29: 180-195.
65. El-Maadawy WH, Hassan M, Hafiz E, Badawy MH, Eldahshan S, AbuSeada A, El-Shazly MAM, Ghareeb MA. Co-treatment with Esculin, isolated from *Vachellia farnesiana*, and erythropoietin attenuates renal ischemia-reperfusion injury via P2X7 receptor and NLRP3 inflammasome inhibition, and PI3K/Akt activation. *Sci Rep* 2022; 12: 6239.
66. Wang Z, Wang C, He B, Zhang W, Liu L, Deng M, Lü M, Qi X, Liang S. Determination of daphnetin and its 8-O-methylated metabolite in rat plasma by UFLC-MS/MS: Application to a pharmacokinetic study. *Chromatographia* 2022; 85: 333-341.

67. Crow FW, Tomer KB, Looker JH, Gross ML. Fast atom bombardment and tandem mass spectrometry for structure determination of steroid and flavonoid glycosides. *Anal Biochem* 1986; 155: 286-307.
68. Tang J, Dunshea FR, Suleria HAR. LC-ESI-QTOF/MS characterization of phenolic compounds from medicinal plants (Hops and Juniper Berries) and their antioxidant activity. *Foods* 2020; 9: 7.
69. Xu M, Zhang Z, Fu G, Sun S, Sun J, Yang M, Liu A, Han J, Guo D. Liquid chromatography-tandem mass spectrometry analysis of protocatechuic aldehyde and its phase I and II metabolites in rat. *J Chromatogr B*. 2007; 856: 100-107.
70. Castillo A, Celeiro M, Lores M, Grgić K, Banožić M, Jerković I, Jokić S. Bioprospecting of targeted phenolic compounds of *Dictyodictyota*, *Gongolariabarbata*, *Ericariaamentacea*, *Sargassum hornschurchii* and *Ellisolandia elongate* from the Adriatic Sea extracted by two green methods. *Mar Drugs* 2023; 21: 97.
71. Zoraghi R, Worrall L, See RH, Strangman W, Popplewell WL, Gong H, Samaai T, Swayze RD, Kaur S, Vuckovic M, Finlay BB, Brunham RC, McMaster WR, Davies-Coleman MT, Strynadka NC, RJ, Reiner NE. Methicillin-resistant *Staphylococcus aureus* (MRSA) pyruvate kinase as a target for bis-indole alkaloids with antibacterial activities. *J Biol Chem* 2011; 286(52): 44716-44725.
72. Chan BC, Ip M, Lau CB, Lui SL, Jolivald C, Ganem-Elbaz C, Litaudon M, Reiner NE, Gong H, See RH, Fung KP, Leung PC. Synergistic effects of baicalein with ciprofloxacin against NorA over-expressed methicillin-resistant *Staphylococcus aureus* (MRSA) and inhibition of MRSA pyruvate kinase. *J Ethnopharmacol* 2011; 137(1): 767-773.
73. Andrade M, Benfeito S, Soares P, e Silva DM, Loureiro J, Borges A, Borges F, Simoes M. Fine-tuning of the hydrophobicity of caffeic acid: studies on the antimicrobial activity against *Staphylococcus aureus* and *Escherichia coli*. *RSC Advances* 2015; 5(66): 53915-53925.
74. Park MY, Kang DH. Antibacterial activity of caffeic acid combined with UV-A light against *Escherichia coli* O157: H7, *Salmonella enterica* serovar Typhimurium, and *Listeria monocytogenes*. *Appl Environ Microbiol* 2021; 87(15): e00631-21.
75. Khan F, Bamunuarachchi NI, Tabassum N, Kim Y.M. Caffeic acid and its derivatives: antimicrobial drugs toward microbial pathogens. *J Agric Food Chem* 2021; 69(10), 2979-3004.